

On the path independence and invariant of the J -integral for a slant crack and rigid-line inclusion using degenerate kernels and the dual BEM

Jeng-Tzong Chen^{a,b,c,d,e,*}, Jeng-Hong Kao^a, Shing-Kai Kao^a, Yi-Ling Huang^a, Yen-Ting Chou^a

^a Department of Harbor and River Engineering, National Taiwan Ocean University, Keelung 20224, Taiwan

^b Department of Mechanical and Mechatronic Engineering, National Taiwan Ocean University, Keelung 20224, Taiwan

^c Department of Civil Engineering, National Cheng-Kung University, Tainan 70101, Taiwan

^d Center of Excellence for Ocean Engineering, National Taiwan Ocean University, Keelung 20224, Taiwan

^e Bachelor Degree Program in Ocean Engineering and Technology, National Taiwan Ocean University, Keelung 20224, Taiwan

ARTICLE INFO

Keywords:

J-integral
Anti-plane shear
Tensor
Crack
Rigid-line inclusion

ABSTRACT

The J -integral and stress intensity factor (SIF) are two major parameters in linear elastic fracture mechanics (LEFM) for the fracture criterion. In this paper, we focus on the J -integral of the slant crack and the slant rigid-line inclusion under the remote anti-plane shear. By employing the degenerate kernel, the path independence of J -integral is analytically demonstrated by using the elliptic coordinates. The positive and negative J -integrals are also analytically derived and numerically implemented by using the dual BEM for the crack and the rigid-line inclusion, respectively. It is interesting to find that the J -integral is not an invariant by using different observer systems but is one component of the vector of the first order tensor. Transformation law of the J -integral with respect to different observers is analytically proved and numerically demonstrated. Finally, the tensor property of order one is examined.

1. Introduction

Line segment problems have been widely investigated using the dual boundary integral equation approach [1]. It has two different boundary conditions in engineering practice in the boundary value problems (BVPs). One is the Dirichlet type and the other is the Neumann type. For the anti-plane elasticity, a rigid-line inclusion is specified by the Dirichlet B.C. to describe the rigid behavior, while a crack is described by the Neumann B.C. to describe the free traction. For the rigid-line inclusion problems, England [2] found that the stress field have singularities near the tip of the rigid-line inclusion in linear elasticity as the same as crack problems. The rigid-line inclusion problems were widely investigated later by either integral equation formulations or numerical testing [3–8]. For the interaction between cracks and rigid-line inclusions, Dong [9] proposed an integral equation approach to investigate the interaction between cracks and rigid-line inclusions embedded in an infinite isotropic elastic matrix subject to the remote loading. Xiao et al. [10] revealed interesting electroelastic interaction phenomena of multiple cracks and multiple rigid-line inclusions by numerical examples.

Wang et al. [11] have summarized a Table for the SIF of the Modes I, II and III for the crack and the rigid inclusion. To determine the value of SIF, three approaches can be employed. One is the extrapolation approach for the boundary or interior displacement near the tip. Another is the extrapolation approach for the boundary stress or interior stress near the tip. The other is the J integral [12] enclosing the crack tip. The J -integral is an efficient way to determine the SIF in energy sense instead of the asymptotic behavior of the displacement or stress near the tip. Whether the J -integral is positive or negative as well as its tensor property attracts the attention of mathematicians and engineers. The popular use of path-independent J -integral lies in the fact that the information regarding the stress and traction states at a discontinuity can be calculated from integrals over a path some distance away from the discontinuity, where singularities are not encountered. Use of contour-integral approach or energy method has the obvious advantage that an accurate modelling of the crack tip behavior is not necessary and accurate results can be obtained by using coarse mesh of boundary elements [13–14]. Then, the use of singular element near the crack tip may not be necessary. Not only for the LEFM, the J -integral

* Corresponding author at: Department of Harbor and River Engineering, National Taiwan Ocean University, Keelung 20224, Taiwan
E-mail address: jtchen@mail.ntou.edu.tw (J.-T. Chen).

approach can be employed with some success as a suitable criterion and can predict the crack growth in the nonlinear and elasto-plastic behavior of cracked bodies. However, the J -integral is not path independent for elasto-plastic materials and is not equal to the energy release rate although it is right for the linear elastic material. Path independence of J -integral is also interesting and can be examined in any observer system. Neglecting the body force, Rice [12] introduced the concept of path-independent J -integral which relates to the energy released per unit of crack translation. In general, there are two components in the J -integral, their component form in different observer systems may not be the same but satisfies the transformation law of tensor of order one. The invariance of J -integral was discussed in the Appendix of Hellan book [15] for the single-valued field. Invariance of the elastodynamic J -integral (J') was also studied by Nishioka [16]. The invariant J -integral in finite element models was also investigated by Ukrainian [17]. Whether the J -integral in the anti-plane elasticity for a slant crack and rigid-line inclusion is an invariant or not attracts our attention.

In this paper, we consider an infinite domain with a slant crack or a slant rigid-line inclusion subject to the remote anti-plane shear case. Therefore, we focus on the SIF of Mode III. Since a crack and a rigid-line inclusion are the special cases of an ellipse, we employ the degenerate kernel in terms of the elliptic coordinates to study this degenerate issue. Thanks to the degenerate kernel, the positive or negative J -integrals and the path independence of J -integral are analytically derived. The numerical experiments by using the dual BEM are also performed. Besides, the transformation law for the component form of J -integral is also analytically and numerically examined. We also proved that results of the horizontal case in [18] are special cases of the present slant cases.

2. Problem statement and mathematical formulation

The J -integral of the horizontal crack and rigid-line inclusion under the anti-plane shear problem have been solved in the [18]. Here, we focus on the J -integral of a slant crack under the anti-plane shear ($\bar{\sigma}_{23}^\infty = S$ and $\bar{\sigma}_{13}^\infty = 0$) or a slant rigid-line inclusion under the anti-plane shear ($\bar{\sigma}_{23}^\infty = 0$ and $\bar{\sigma}_{13}^\infty = S$) as shown in Fig. 1. The J -integral defined by Rice [12] was given below:

$$J_{x_1} = \int_{\Gamma} \left(W n_1 - T_i \frac{\partial u_i}{\partial x_1} \right) d\Gamma, \quad (1)$$

where Γ is the path along which the J -integral is calculated, $W = \frac{\sigma_{ij}\epsilon_{ij}}{2}$ is the strain energy density for the linear elastic material, n_1 is the component of the outward unit normal \mathbf{n} in the first direction x_1 , u_i is the i th component of the displacement vector and $T_i = \sigma_{ij}n_j$ is the traction along Γ , respectively, and $d\Gamma$ is the differential arc length. For the anti-plane problem, the nonvanishing shear strains are given by

$$\epsilon_{13} = \frac{1}{2} \frac{\partial u_3}{\partial x_1}, \quad \epsilon_{23} = \frac{1}{2} \frac{\partial u_3}{\partial x_2}, \quad (2)$$

and the corresponding stresses follow Hooke's law as

$$\sigma_{13} = 2\mu\epsilon_{13}, \quad \sigma_{23} = 2\mu\epsilon_{23}, \quad (3)$$

where μ is the shear modulus. Therefore, the strain energy density is given by

$$W = \sigma_{13}\epsilon_{13} + \sigma_{23}\epsilon_{23} = \frac{\sigma_{13}^2 + \sigma_{23}^2}{2\mu}. \quad (4)$$

The traction is

$$T_3 = \sigma_{13}n_1 + \sigma_{23}n_2. \quad (5)$$

By substituting Eq. (2) into Eq. (3), we have

$$\frac{\partial u_3}{\partial x_1} = \frac{\sigma_{13}}{\mu}, \quad \frac{\partial u_3}{\partial x_2} = \frac{\sigma_{23}}{\mu}. \quad (6)$$

For a slant crack or a slant rigid-line inclusion, the J -integral can be derived by two different observer systems. One is that we can decompose it into the combination of two horizontal cases under the different remote anti-plane shear since the observer system is attached on the crack or rigid-line inclusion as shown in Fig. 1. The other is using the observer system subject to the original system coordinates, (\bar{x}_1, \bar{x}_2) . Fig. 2 shows a slant crack and a slant rigid-line inclusion by using the (x_1, x_2) observer coordinate system while Fig. 3 shows the (\bar{x}_1, \bar{x}_2) system. Here, we focus on the J -integral derived by using the (x_1, x_2) observer coordinate system.

To derive the J -integral, we need to solve the total displacement first. Hence, we introduce the degenerate kernel. By employing the degenerate kernel, the collocation point can be located on the real boundary free of the singular integral. Therefore, the representations of integral equations and null-field integral equations including the boundary point for the exterior problem can be written as

$$2\pi u(\mathbf{x}) = \int_B T^e(\mathbf{s}, \mathbf{x})u(\mathbf{s})dB(\mathbf{s}) - \int_B U^e(\mathbf{s}, \mathbf{x})t(\mathbf{s})dB(\mathbf{s}), \quad \mathbf{x} \in D \cup B, \quad (7)$$

$$2\pi t(\mathbf{x}) = \int_B M^e(\mathbf{s}, \mathbf{x})u(\mathbf{s})dB(\mathbf{s}) - \int_B L^e(\mathbf{s}, \mathbf{x})t(\mathbf{s})dB(\mathbf{s}), \quad \mathbf{x} \in D \cup B, \quad (8)$$

and

$$0 = \int_B T^i(\mathbf{s}, \mathbf{x})u(\mathbf{s})dB(\mathbf{s}) - \int_B U^i(\mathbf{s}, \mathbf{x})t(\mathbf{s})dB(\mathbf{s}), \quad \mathbf{x} \in D^c \cup B, \quad (9)$$

$$0 = \int_B M^i(\mathbf{s}, \mathbf{x})u(\mathbf{s})dB(\mathbf{s}) - \int_B L^i(\mathbf{s}, \mathbf{x})t(\mathbf{s})dB(\mathbf{s}), \quad \mathbf{x} \in D^c \cup B, \quad (10)$$

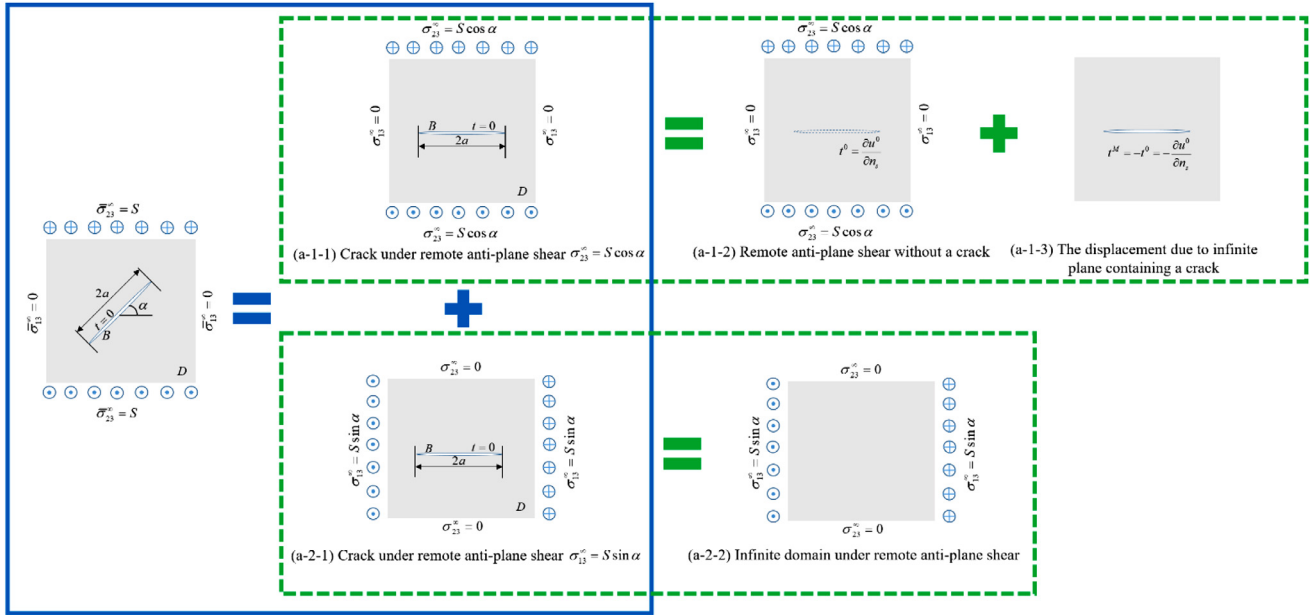
respectively, where D is the domain, D^c is the complementary domain, B is the boundary and the degenerate kernel in the dual BIEM will be elaborated on later. Since the anti-plane problem satisfies the Laplace equation, the closed-form fundamental solution in the BEM/BIEM is $U(\mathbf{s}, \mathbf{x}) = \ln |\mathbf{x} - \mathbf{s}| = \ln r$, where r is the distance between \mathbf{x} and \mathbf{s} . By employing the separable property of the kernel, $U(\mathbf{s}, \mathbf{x})$ can be expanded into the series form by separating the source point and the field point. Since the crack and the rigid-line inclusion problem is a degenerate case of an ellipse, we express the degenerate kernel in terms of elliptic coordinates [19–21] as shown below:

$$U(\mathbf{s}, \mathbf{x}) = \begin{cases} U^i(\xi_s, \eta_s; \xi_x, \eta_x) = \xi_s + \ln \frac{c}{2} - \sum_{m=1}^{\infty} \frac{2}{m} e^{-m\xi_s} \cosh m\xi_x \cos m\eta_x \cos m\eta_s \\ \quad - \sum_{m=1}^{\infty} \frac{2}{m} e^{-m\xi_s} \sinh m\xi_x \sin m\eta_x \sin m\eta_s, \quad \xi_s \geq \xi_x, \quad (a) \\ U^e(\xi_s, \eta_s; \xi_x, \eta_x) = \xi_x + \ln \frac{c}{2} - \sum_{m=1}^{\infty} \frac{2}{m} e^{-m\xi_s} \cosh m\xi_s \cos m\eta_x \cos m\eta_s \\ \quad - \sum_{m=1}^{\infty} \frac{2}{m} e^{-m\xi_s} \sinh m\xi_s \sin m\eta_x \sin m\eta_s, \quad \xi_s < \xi_x, \quad (b) \end{cases} \quad (11)$$

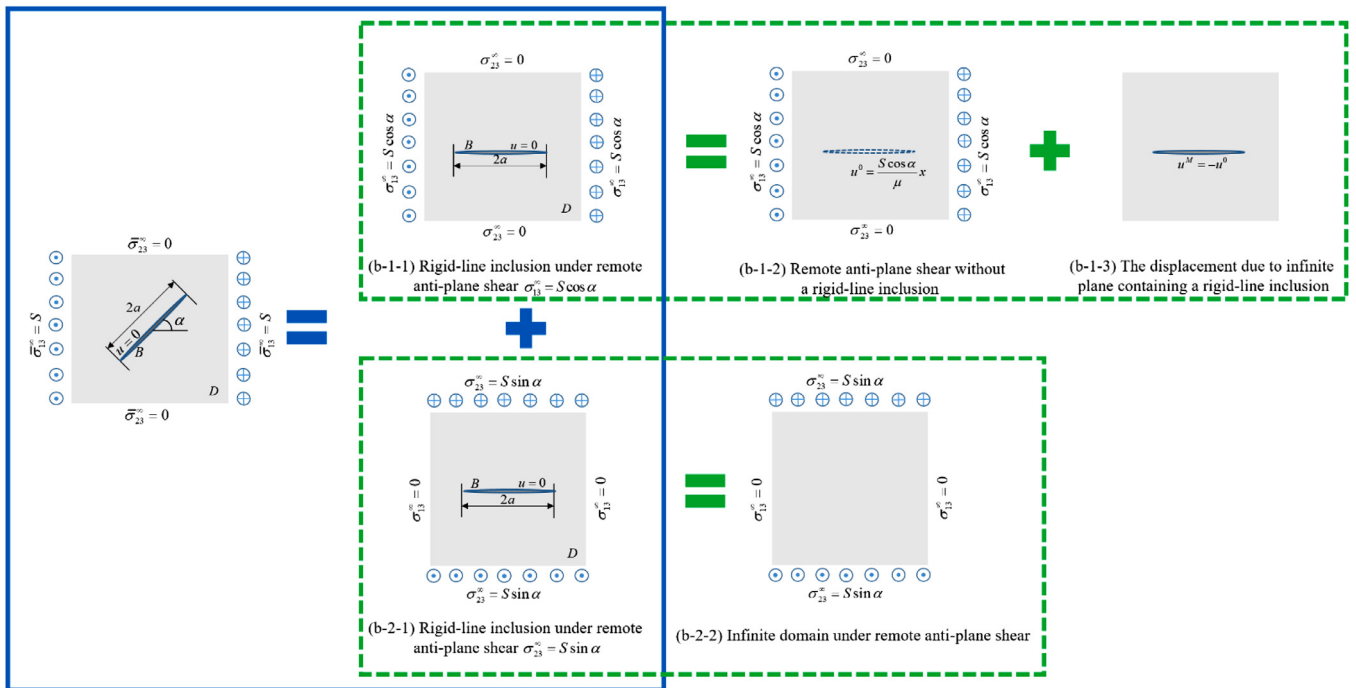
where the field point $\mathbf{x} = (\xi_x, \eta_x)$, the source point $\mathbf{s} = (\xi_s, \eta_s)$, and c is the half distance between two foci, the superscripts “ i ” and “ e ” denote the interior ($\xi_s \geq \xi_x$) and exterior ($\xi_s < \xi_x$) cases, respectively. The degenerate-kernel expression for the closed-form fundamental solution of $U(\mathbf{s}, \mathbf{x})$ is shown in Fig. 4. After taking the normal derivative $-\partial/\partial n_s$ with respect to the source point, $T(\mathbf{s}, \mathbf{x})$ can be obtained as shown below:

$$T(\mathbf{s}, \mathbf{x}) = \begin{cases} T^i(\xi_s, \eta_s; \xi_x, \eta_x) = \frac{-1}{J(\xi_s, \eta_s)} \left(1 + 2 \sum_{m=1}^{\infty} e^{-m\xi_s} \cosh m\xi_x \cos m\eta_x \cos m\eta_s \right. \\ \quad \left. + 2 \sum_{m=1}^{\infty} e^{-m\xi_s} \sinh m\xi_x \sin m\eta_x \sin m\eta_s \right), \quad \xi_s > \xi_x, \quad (a) \\ T^e(\xi_s, \eta_s; \xi_x, \eta_x) = \frac{1}{J(\xi_s, \eta_s)} \left(2 \sum_{m=1}^{\infty} e^{-m\xi_s} \sinh m\xi_s \cos m\eta_x \cos m\eta_s \right. \\ \quad \left. + 2 \sum_{m=1}^{\infty} e^{-m\xi_s} \cosh m\xi_s \sin m\eta_x \sin m\eta_s \right), \quad \xi_s < \xi_x. \quad (b) \end{cases} \quad (12)$$

It is noted that a Jacobian term, $J(\xi_s, \eta_s) = J_s = c\sqrt{\cosh^2 \xi_s \sin^2 \eta_s + \sinh^2 \xi_s \cos^2 \eta_s}$, is in the denominator.



(a) A slant crack under the remote anti-plane shear ($\bar{\sigma}_{23}^{\infty} = S$ and $\bar{\sigma}_{13}^{\infty} = 0$)



(b) A slant rigid-line inclusion under the remote anti-plane shear ($\bar{\sigma}_{23}^{\infty} = 0$ and $\bar{\sigma}_{13}^{\infty} = S$)

Fig. 1. Orientation and decomposition of a slant crack and a slant rigid-line inclusion.

3. Analytical derivation of the path independence of J -integral

Now, we consider the slant crack under the anti-plane shear ($\bar{\sigma}_{23}^{\infty} = S$ and $\bar{\sigma}_{13}^{\infty} = 0$) as shown in Fig. 1(a), where α is the inclined angle of the crack. The problem can be decomposed into two horizontal cases as shown in Fig. 1(a-1-1) and 1(a-2-1) by employing the superposition technique. However, the total displacement in Fig. 1(a-1-1) can be decomposed again as Fig. 1(a-1-2) and 1(a-1-3) while Fig. 1(a-2-1) is equal to Fig. 1(a-2-2) since a crack is trivial here. Fig. 1(a-1-2) and 1(a-2-2)

are both due to the remote shear loading u^{∞} in an infinite plane. The displacement of $u^M(\mathbf{x})$ is caused by the infinite plane problem with a crack as shown in Fig. 1(a-1-3). The boundary condition on the crack is free of traction, which yields the Neumann boundary condition. Since u^{∞} is given, the $t^M(\mathbf{s})$ on the crack surface can be obtained. By applying the Fourier expansions, the specified boundary data $u^M(\mathbf{s})$ can be expressed. By using Eq. (9), the unknown boundary density $u^M(\mathbf{s})$ can be obtained after comparing coefficients of the basis. By solving the Fig. 1(a-1-3) using the BIE, the total displacement of the slant crack

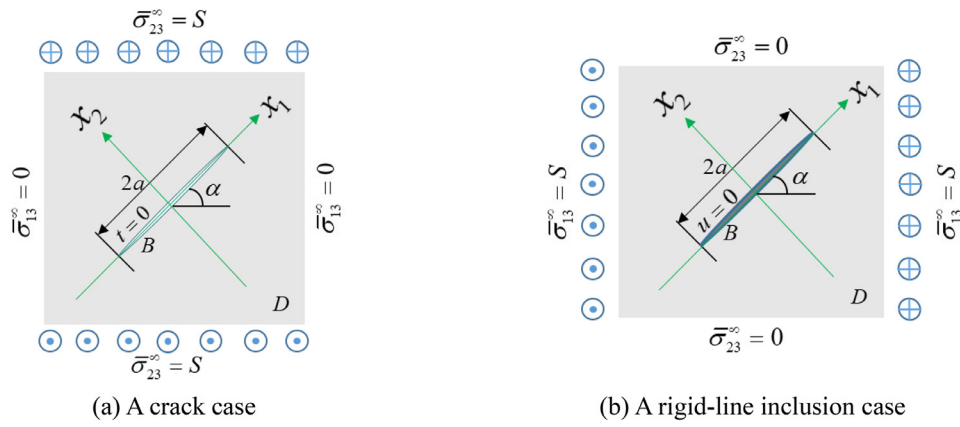


Fig. 2. A slant crack and a slant rigid-line inclusion by using the (x_1, x_2) observer coordinate system. (a) A crack case. (b) A rigid-line inclusion case.

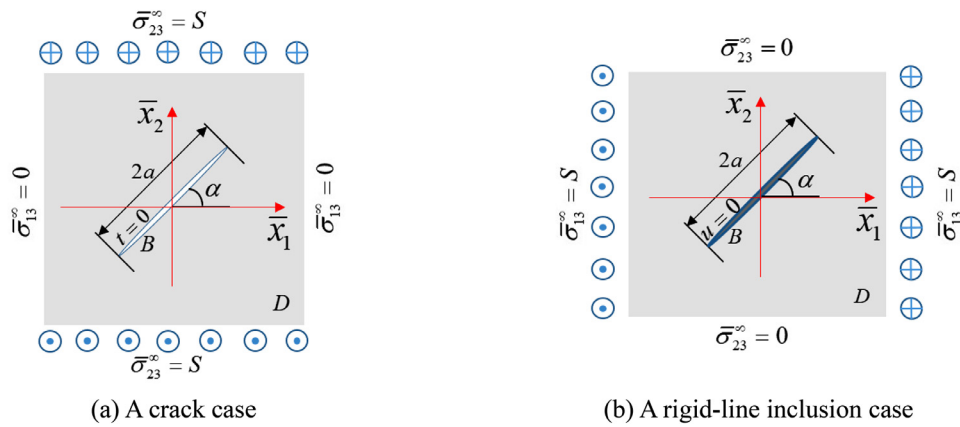


Fig. 3. A slant crack and a slant rigid-line inclusion by using the (\bar{x}_1, \bar{x}_2) observer coordinate system. (c) A crack case. (d) A rigid-line inclusion case.

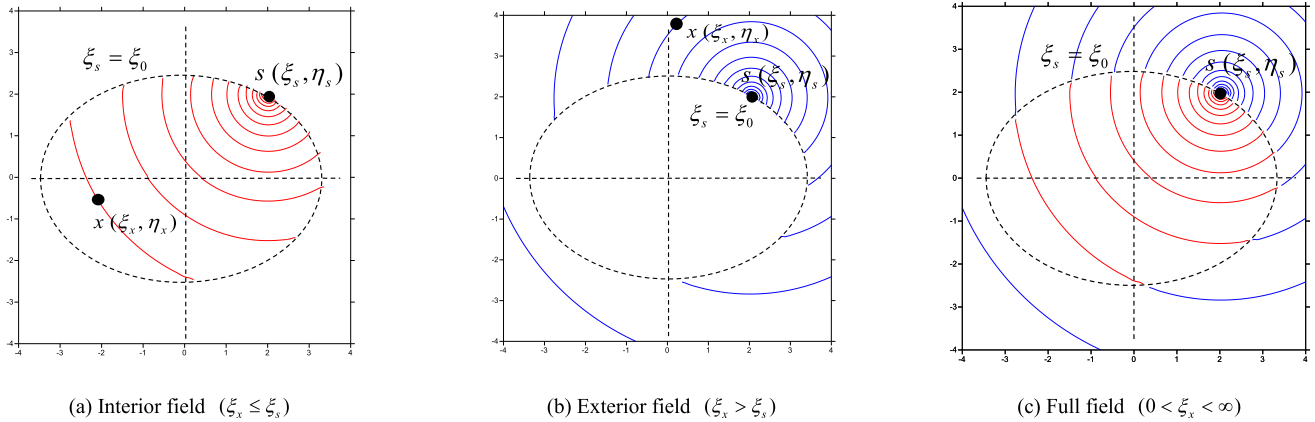


Fig. 4. Contour plot of the degenerate kernel for the fundamental solution $(U(s, x))$ in elliptic coordinates, $\xi_s = \xi_0$.

yields

$$u_3(\xi_x, \eta_x) = \frac{S}{\mu} c (\sin \eta_x \cosh \xi_x \cos \alpha + \cos \eta_x \cosh \xi_x \sin \alpha). \quad (13)$$

The stress is

$$\sigma_{13} = \mu \left(h_1 \frac{\partial u_3}{\partial \xi_x} - h_2 \frac{\partial u_3}{\partial \eta_x} \right) = \frac{S c^2 (-\sin \eta_x \cos \eta_x \cos \alpha)}{J_x^2} + S \sin \alpha, \quad (14)$$

$$\sigma_{23} = \mu \left(h_2 \frac{\partial u_3}{\partial \xi_x} + h_1 \frac{\partial u_3}{\partial \eta_x} \right) = \frac{S c^2 \cosh \xi_x \sinh \xi_x \cos \alpha}{J_x^2}, \quad (15)$$

where $h_1 = \frac{\sinh \xi_x \cos \eta_x}{c((\sinh \xi_x \cos \eta_x)^2 + (\cosh \xi_x \sin \eta_x)^2)}$, $h_2 = \frac{\cosh \xi_x \sin \eta_x}{c((\sinh \xi_x \cos \eta_x)^2 + (\cosh \xi_x \sin \eta_x)^2)}$

and $J_x = c \sqrt{\cosh^2 \xi_x \sin^2 \eta_x + \sinh^2 \xi_x \cos^2 \eta_x}$. By substituting Eqs. (14) and (15) into Eq (4), the strain energy density yields

$$W = \frac{S^2 c^2}{2\mu} \left(\frac{\cos^2 \eta_x + \sinh^2 \xi_x}{J_x^2} \right) \cos^2 \alpha - \frac{2S^2 c^2}{2\mu} \left(\frac{\sin \eta_x \cos \eta_x}{J_x^2} \right) \sin \alpha \cos \alpha + \frac{S^2}{2\mu} \sin^2 \alpha \quad (16)$$

since the total displacement is obtained. The integral path is decomposed of three parts, Γ_1, Γ_2 and Γ_3 in Table 1. The component of the

Table 1
Stress intensity factor of the slant crack under the anti-plane shear.

Approach	Observation point		
	Boundary data	Interior field	Field and boundary
Displacement	$K_{III} = \lim_{\epsilon \rightarrow 0} \frac{\mu \sqrt{\pi a} u_3(0, \eta_\epsilon)}{\sqrt{2\epsilon}} = S \cos \alpha \sqrt{\pi a}$	$K_{III} = \lim_{\epsilon \rightarrow 0} \frac{\mu \sqrt{\pi a} u_3(\xi_\epsilon, 0)}{\sqrt{2\epsilon}} = S \cos \alpha \sqrt{\pi a}$	
Stress	$K_{IIIx} = \lim_{\epsilon \rightarrow 0} \sqrt{2\pi\epsilon} \sigma(0, \eta) = S \cos \alpha \sqrt{\pi a}$	$K_{IIIx} = \lim_{\epsilon \rightarrow 0} \sqrt{2\pi\epsilon} \sigma(\xi, 0) = S \cos \alpha \sqrt{\pi a}$	
J-integral			$J_{x_1}^{ca} = \frac{S^2 \pi a}{2\mu} \cos^2 \alpha = \frac{K_{III}^2}{2\mu}$

outward unit normal vector \mathbf{n} for the elliptic contour Γ_2 ($\xi_x = \xi_1$) is

$$n_1 = \frac{\sinh \xi_x \cos \eta_x}{\sqrt{(\sinh \xi_x \cos \eta_x)^2 + (\cosh \xi_x \sin \eta_x)^2}}, \tag{17}$$

$$n_2 = \frac{\cosh \xi_x \sin \eta_x}{\sqrt{(\sinh \xi_x \cos \eta_x)^2 + (\cosh \xi_x \sin \eta_x)^2}}. \tag{18}$$

For the elliptic coordinates, we have $a = c \cosh \xi_x$ and $b = c \sinh \xi_x$, where a is the semi-major axis and b is the semi-minor axis of the ellipse. Eqs. (17) and (18) can be written as

$$n_1 = \frac{b \cos \eta_x}{J_x}, \tag{19}$$

$$n_2 = \frac{a \sin \eta_x}{J_x}. \tag{20}$$

By substituting Eqs. (14), (15), (19) and (20) into Eq. (5), we have

$$T_3 = \frac{Sc \sinh \xi_x (\sin \eta_x \cos \alpha + \sin \alpha \cos \eta_x)}{J_x}. \tag{21}$$

By substituting Eq. (14) into Eq. (6), we have

$$\frac{\partial u_3}{\partial x_1} = \frac{Sc^2 (-\sin \eta_x \cos \eta_x \cos \alpha)}{\mu J_x^2} + \frac{S \sin \alpha}{\mu}. \tag{22}$$

By substituting Eqs. (16), (19), (21) and (22) into Eq. (1), the J -integral for the contour Γ_2 yields

$$\begin{aligned} (J_{x_1}^{ca})_{\Gamma_2} &= \int_{\Gamma_2} \left(\frac{S^2 c^2 b \cos \eta_x \cos^2 \alpha}{2\mu J_x^3} + \frac{S^2 b \cos \eta_x}{2\mu J_x} (\cos^2 \alpha - \sin^2 \alpha) \right. \\ &\quad \left. + \frac{S^2 b \sin \eta_x \cos \alpha \sin \alpha}{\mu J_x} \right) J_x d\eta_x \\ &= \frac{S^2 c \cos^2 \alpha}{\mu} \left(\tan^{-1} \frac{1}{\sinh \xi_1} \right) + \frac{S^2 b}{\mu} (\cos^2 \alpha - \sin^2 \alpha). \end{aligned} \tag{23}$$

However, the component of the outward unit normal vector \mathbf{n} for the contour Γ_1 ($0 < \xi_x < \xi_1$) and Γ_3 ($0 < \xi_x < \xi_1$) is

$$n_1 = -1, \quad n_2 = 0. \tag{24}$$

Therefore, we have

$$W n_1 = \left(\frac{S^2 c^2}{2\mu} \left(\frac{\cos^2 \eta_x + \sinh^2 \xi_x}{J_x^2} \right) \right) \cos^2 \alpha$$

$$\begin{aligned} & - \frac{2S^2 c^2}{2\mu} \left(\frac{\sin \eta_x \cos \eta_x}{J_x^2} \right) \sin \alpha \cos \alpha + \frac{S^2}{2\mu} \sin^2 \alpha \tag{25} \\ & = - \frac{S^2 c^2 \cos^2 \eta_x \cos^2 \alpha}{2\mu J_x^2} - \frac{S^2 c^2 \sinh^2 \xi_x \cos^2 \alpha}{2\mu J_x^2} \\ & \quad + \frac{S^2 c^2 \sin \eta_x \cos \eta_x \sin \alpha \cos \alpha}{\mu J_x^2} - \frac{S^2}{2\mu} \sin^2 \alpha, \end{aligned}$$

$$\begin{aligned} T_3 \frac{\partial u_3}{\partial x_1} &= \left(\frac{Sc^2 (-\sin \eta_x \cos \eta_x \cos \alpha)}{J_x^2} + S \sin \alpha \right) (-1) \\ &\quad \times \left(\frac{Sc^2 (-\sin \eta_x \cos \eta_x \cos \alpha)}{J_x^2} + S \sin \alpha \right) \frac{1}{\mu} \\ &= - \frac{1}{\mu} \left(\frac{Sc^2 (-\sin \eta_x \cos \eta_x \cos \alpha)}{J_x^2} + S \sin \alpha \right)^2. \end{aligned} \tag{26}$$

By substituting Eqs. (25) and (26) into Eq. (1) for $d\Gamma = -c \cosh \xi_x \sin \eta_x d\xi_x$ and by substituting $\eta_x = -\frac{\pi}{2}$ and $\eta_x = \frac{\pi}{2}$ for the contour Γ_1 and Γ_3 , respectively, the J -integrals for the contours Γ_1 and Γ_3 yield

$$\begin{aligned} (J_{x_1}^{ca})_{\Gamma_1} &= \int_{\Gamma_1} \left(-\frac{S^2 \sinh^2 \xi_x}{2\mu \cosh^2 \xi_x} \cos^2 \alpha + \frac{S^2}{2\mu} \sin^2 \alpha \right) (c \cosh \xi_x d\xi_x) \\ &= -\frac{S^2 b}{2\mu} \cos^2 \alpha + \frac{S^2 c}{2\mu} \cos^2 \alpha (\tan^{-1} \sinh \xi_1) + \frac{S^2 b}{2\mu} \sin^2 \alpha, \end{aligned} \tag{27}$$

$$\begin{aligned} (J_{x_1}^{ca})_{\Gamma_3} &= \int_{\Gamma_3} \left(-\frac{S^2 \sinh^2 \xi_x}{2\mu \cosh^2 \xi_x} \cos^2 \alpha + \frac{S^2}{2\mu} \sin^2 \alpha \right) (-c \cosh \xi_x d\xi_x) \\ &= -\frac{S^2 b}{2\mu} \cos^2 \alpha + \frac{S^2 c}{2\mu} \cos^2 \alpha (\tan^{-1} \sinh \xi_1) + \frac{S^2 b}{2\mu} \sin^2 \alpha, \end{aligned} \tag{28}$$

respectively. It is interesting to find that Γ_1 and Γ_3 contribute to the same weight for the J -integral. Therefore, the J -integral for the contour Γ can be obtained as

$$J_{x_1}^{ca} = \frac{S^2 c \pi}{2\mu} \cos^2 \alpha, \tag{29}$$

where $c = a$ in the degenerate case. Eq. (29) can be rewritten as

$$J_{x_1}^{ca} = \frac{S^2 \pi a}{2\mu} \cos^2 \alpha. \tag{30}$$

Table 2
 J_{x_1} and J_{x_2} of the crack under the anti-plane shear.

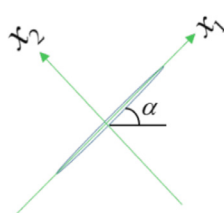
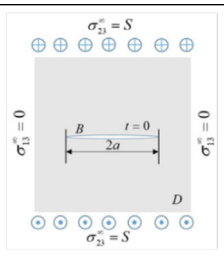
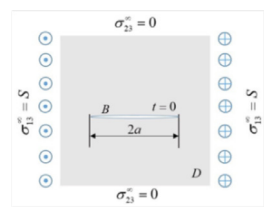
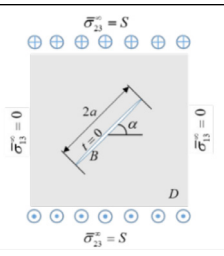
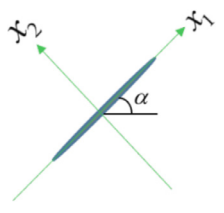
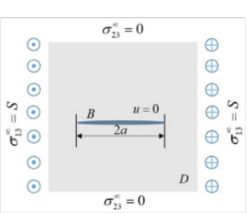
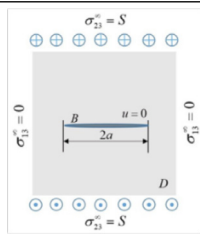
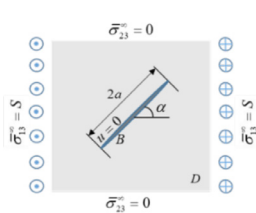
Observer system (x_1, x_2)	Crack	Crack (trivial)	Slant crack
			
J_{x_1} J_{x_2}	$\frac{S^2 \pi a}{2\mu}$ 0	0 0	$\frac{S^2 \pi a}{2\mu} \cos^2 \alpha$ $-\frac{S^2 a}{\mu} \sin 2 \alpha$

Table 3
 J_{x_1} and J_{x_2} of the rigid-line inclusion under the anti-plane shear.

Observer system (x_1, x_2)	Crack	Crack (trivial)	Slant crack
			
J_{x_1} J_{x_2}	$-\frac{S^2 \pi a}{2\mu}$ 0	0 0	$-\frac{S^2 \pi a}{2\mu} \cos^2 \alpha$ $\frac{S^2 a}{\mu} \sin 2 \alpha$

However, the SIF can be derived from three ways. One is the J -integral, another is the asymptotic behavior on the interior or boundary stress near the crack tip and the other is displacement fields of the asymptotic behavior on the interior or boundary near the crack tip of [22]. Following the similar procedure in [18], the SIF of the slant crack can be derived from the asymptotic behavior. Here, we only show the final result in Table 1. The SIF yields

$$K_{III} = S \sqrt{\pi a} \cos \alpha. \tag{31}$$

Eq. (31) also yields the same result in [23]. Hence, Eq. (30) can be written as

$$J_{x_1}^{ca} = \frac{K_{III}^2}{2\mu}. \tag{32}$$

Eq. (32) yields the same result as mentioned in [18, 24-26]. The path independence of J -integral is also proved.

According to the definition of J -integral, it is a tensor of order one. Here, we find that the J -integral defined by Rice is only the x_1 component while the x_2 component is given by

$$J_{x_2} = \int_{\Gamma} \left(W n_2 - T_i \frac{\partial u_i}{\partial x_2} \right) d\Gamma. \tag{33}$$

Therefore, we have

$$\begin{aligned} (J_{x_2}^{ca})_{\Gamma_2} &= \int_{\Gamma_2} \left(\frac{S^2 c^2}{2\mu} \frac{a \sin \eta_x}{J_x^3} \cos^2 \alpha + \frac{S^2}{2\mu} \frac{a \sin \eta_x}{J_x} (\sin^2 \alpha - \cos^2 \alpha) \right. \\ &\quad \left. - \frac{S^2}{\mu} \frac{a \cos \eta_x \sin \alpha \cos \alpha}{J_x} \right) J_x d\eta_x \\ &= -\frac{2S^2}{\mu} c \sin \alpha \cos \alpha \cosh \xi_1, \end{aligned} \tag{34}$$

for the contour Γ_2 . For the contours Γ_1 and Γ_3 , we have

$$(J_{x_2}^{ca})_{\Gamma_1} = \int_{\Gamma_1} \left(\frac{S^2 c^2 \cosh \xi_x \sinh \xi_x \sin \alpha \cos \alpha}{\mu J_x^2} \right) (c \cosh \xi_x d\xi_x)$$

$$= \frac{S^2 c}{\mu} \sin \alpha \cos \alpha \cosh \xi_1 - \frac{S^2 c}{\mu} \sin \alpha \cos \alpha, \tag{35}$$

$$\begin{aligned} (J_{x_2}^{ca})_{\Gamma_3} &= \int_{\Gamma_3} \left(\frac{S^2 c^2 \cosh \xi_x \sinh \xi_x \sin \alpha \cos \alpha}{\mu J_x^2} \right) (-c \cosh \xi_x d\xi_x) \\ &= \frac{S^2 c}{\mu} \sin \alpha \cos \alpha \cosh \xi_1 - \frac{S^2 c}{\mu} \sin \alpha \cos \alpha, \end{aligned} \tag{36}$$

respectively. After combining the integrals for Γ_1, Γ_2 and Γ_3 , we have

$$J_{x_2}^{ca} = \frac{-S^2 a}{\mu} \sin 2\alpha. \tag{37}$$

for the slant crack. Similarly, we have

$$J_{x_1}^{ia} = \frac{-S^2 \pi a}{2\mu} \cos^2 \alpha = -\frac{K_{III}^2}{2\mu}, \tag{38}$$

$$J_{x_2}^{ia} = \frac{S^2 a}{\mu} \sin 2\alpha, \tag{39}$$

for the slant rigid-line inclusion. Eq. (38) can be also obtained by using the Eq. (32) since the reciprocal relation for the SIF between a crack and a rigid-line inclusion with respect to the opposite loading was addressed in [18], which is an extension of the reciprocal relation for the SCF between a hole and a rigid inclusion [13,27-28]. After comparing Eqs. (30) and (35) with Eqs. (38) and (39) for the crack and rigid-line inclusion, their results are different by a sign. From Eqs. (37) and (39), we also find that J_{x_2} is also path independent no matter what ξ_0 is. The results of J_{x_2} for the horizontal crack and horizontal rigid-line inclusion are both derived by setting $\alpha = 0$ although J_{x_1} was obtained in [18]. According to the definition, we summarize the result of J_{x_1} and J_{x_2} for the crack in Table 2 while the result of the rigid-line inclusion is shown in Table 3. It also indicates that the result in [18] is the special case of the present paper by setting $\alpha = 0, \frac{\pi}{2}, \pi$ and $\frac{3\pi}{2}$. It is found that J_{x_1} are positive and negative for the crack and the rigid-line inclusion, respectively,

Table 4
First order tensor of J -integral in the (x_1, x_2) and (\bar{x}_1, \bar{x}_2) observer system for the rigid-line inclusion.

	<p>Transformation law</p>	
$u_3(x_1, x_2)$	$u_3(x_1, x_2) = \bar{u}_3(\bar{x}_1, \bar{x}_2)$	$\bar{u}_3(\bar{x}_1, \bar{x}_2)$
$\frac{\partial u_3}{\partial x_1}$	$\begin{bmatrix} \frac{\partial \bar{u}_3}{\partial \bar{x}_1} \\ \frac{\partial \bar{u}_3}{\partial \bar{x}_2} \end{bmatrix} = \begin{bmatrix} \cos \alpha & -\sin \alpha \\ \sin \alpha & \cos \alpha \end{bmatrix} \begin{bmatrix} \frac{\partial u_3}{\partial x_1} \\ \frac{\partial u_3}{\partial x_2} \end{bmatrix}$	$\frac{\partial \bar{u}_3}{\partial \bar{x}_1} = \left(\frac{\partial u_3}{\partial x_1} \cos \alpha - \frac{\partial u_3}{\partial x_2} \sin \alpha \right)$
$\frac{\partial u_3}{\partial x_2}$		$\frac{\partial \bar{u}_3}{\partial \bar{x}_2} = \left(\frac{\partial u_3}{\partial x_1} \sin \alpha + \frac{\partial u_3}{\partial x_2} \cos \alpha \right)$
$\sigma_{13} = \mu \frac{\partial u_3}{\partial x_1}$	$\begin{bmatrix} \bar{\sigma}_{13} \\ \bar{\sigma}_{23} \end{bmatrix} = \begin{bmatrix} \cos \alpha & -\sin \alpha \\ \sin \alpha & \cos \alpha \end{bmatrix} \begin{bmatrix} \sigma_{13} \\ \sigma_{23} \end{bmatrix}$	$\bar{\sigma}_{13} = \mu \frac{\partial \bar{u}_3}{\partial \bar{x}_1} = \mu \left(\frac{\partial u_3}{\partial x_1} \cos \alpha - \frac{\partial u_3}{\partial x_2} \sin \alpha \right)$
$\sigma_{23} = \mu \frac{\partial u_3}{\partial x_2}$		$\bar{\sigma}_{23} = \mu \frac{\partial \bar{u}_3}{\partial \bar{x}_2} = \mu \left(\frac{\partial u_3}{\partial x_1} \sin \alpha + \frac{\partial u_3}{\partial x_2} \cos \alpha \right)$
$n = (\cos \beta, \sin \beta)$	$\begin{bmatrix} \bar{n}_1 \\ \bar{n}_2 \end{bmatrix} = \begin{bmatrix} \cos \alpha & -\sin \alpha \\ \sin \alpha & \cos \alpha \end{bmatrix} \begin{bmatrix} n_1 \\ n_2 \end{bmatrix}$	$\bar{n} = (\cos(\alpha + \beta), \sin(\alpha + \beta))$
$W = \frac{\sigma_{13}^2 + \sigma_{23}^2}{2\mu} = \frac{\mu}{2} \left(\left(\frac{\partial u_3}{\partial x_1} \right)^2 + \left(\frac{\partial u_3}{\partial x_2} \right)^2 \right)$	$W = \bar{W}$	$\bar{W} = \frac{\bar{\sigma}_{13}^2 + \bar{\sigma}_{23}^2}{2\mu} = \frac{\mu}{2} \left(\left(\frac{\partial \bar{u}_3}{\partial \bar{x}_1} \right)^2 + \left(\frac{\partial \bar{u}_3}{\partial \bar{x}_2} \right)^2 \right) = W$
$T_3 = \sigma_{13} n_1 + \sigma_{23} n_2 = \mu \left(\frac{\partial u_3}{\partial x_1} \cos \beta + \frac{\partial u_3}{\partial x_2} \sin \beta \right)$	$T_3 = \bar{T}_3$	$\bar{T}_3 = \bar{\sigma}_{13} \bar{n}_1 + \bar{\sigma}_{23} \bar{n}_2 = \mu \left(\frac{\partial u_3}{\partial x_1} \cos \beta + \frac{\partial u_3}{\partial x_2} \sin \beta \right) = T_3$
$J_{x_1}^{ia} = \int_{\Gamma} W n_1 - T_3 \frac{\partial u_3}{\partial x_1} d\Gamma$ $= \int_{\Gamma} \frac{\mu}{2} \left(- \left(\frac{\partial u_3}{\partial x_1} \right)^2 \cos \beta + \left(\frac{\partial u_3}{\partial x_2} \right)^2 \cos \beta - 2 \frac{\partial u_3}{\partial x_1} \frac{\partial u_3}{\partial x_2} \sin \beta \right) d\Gamma$	$\begin{bmatrix} J_{x_1}^{ia} \\ J_{x_2}^{ia} \end{bmatrix} = \begin{bmatrix} \cos \alpha & -\sin \alpha \\ \sin \alpha & \cos \alpha \end{bmatrix} \begin{bmatrix} J_{x_1}^{ia} \\ J_{x_2}^{ia} \end{bmatrix}$ $\left(J_{x_1}^{ia} \right)^2 + \left(J_{x_2}^{ia} \right)^2 = \left(J_{x_1}^{ia} \right)^2 + \left(J_{x_2}^{ia} \right)^2$	$J_{x_1}^{ia} = \int_{\Gamma} \bar{W} \bar{n}_1 - \bar{T}_3 \frac{\partial \bar{u}_3}{\partial \bar{x}_1} d\Gamma$ $= \int_{\Gamma} \frac{\mu}{2} \left(- \left(\frac{\partial u_3}{\partial x_1} \right)^2 \cos(\beta - \alpha) + \left(\frac{\partial u_3}{\partial x_2} \right)^2 \cos(\beta - \alpha) - 2 \frac{\partial u_3}{\partial x_1} \frac{\partial u_3}{\partial x_2} \sin(\beta - \alpha) \right) d\Gamma$
$J_{x_2}^{ia} = \int_{\Gamma} W n_2 - T_3 \frac{\partial u_3}{\partial x_2} d\Gamma$ $= \int_{\Gamma} \frac{\mu}{2} \left(\left(\frac{\partial u_3}{\partial x_1} \right)^2 \sin \beta - \left(\frac{\partial u_3}{\partial x_2} \right)^2 \sin \beta - 2 \frac{\partial u_3}{\partial x_1} \frac{\partial u_3}{\partial x_2} \cos \beta \right) d\Gamma$		$J_{x_2}^{ia} = \int_{\Gamma} \bar{W} \bar{n}_2 - \bar{T}_3 \frac{\partial \bar{u}_3}{\partial \bar{x}_2} d\Gamma$ $= \int_{\Gamma} \frac{\mu}{2} \left(\left(\frac{\partial u_3}{\partial x_1} \right)^2 \sin(\beta - \alpha) - \left(\frac{\partial u_3}{\partial x_2} \right)^2 \sin(\beta - \alpha) - 2 \frac{\partial u_3}{\partial x_1} \frac{\partial u_3}{\partial x_2} \cos(\beta - \alpha) \right) d\Gamma$

not only for the horizontal but also for the slant case. However, J_{x_2} are negative and positive for the crack and the rigid-line inclusion, respectively. It is interesting to find that $J_{x_2} = 0$ when $\alpha = 0, \frac{\pi}{2}, \pi$ and $\frac{3\pi}{2}$. This indicates that J_{x_2} only makes a contribution in the slant case. Although only the anti-plane shear loading case is considered, the extension work to the in-plane loading is straightforward and related works can be found in [29-30].

4. On the tensor property of J -integral

Since the J -integral is a tensor of order one, we examine the tensor property of the J -integral for the slant rigid-line inclusion here. Two observer systems are used. Not only the analytical solutions but also

numerical evidences are done here. The observer coordinates system (x_1, x_2) is counter colockwise rotated by α angle with respect to the (\bar{x}_1, \bar{x}_2) system as shown in Table 4. We choose a circular path to examine the tensor property, the normal vector of the integral-path in the (x_1, x_2) system as shown in Table 4(a) is

$$n = (\cos \beta, \sin \beta). \tag{40}$$

The strain energy density and the traction along Γ are

$$W = \frac{\sigma_{13}^2 + \sigma_{23}^2}{2\mu} = \frac{\mu}{2} \left(\left(\frac{\partial u_3}{\partial x_1} \right)^2 + \left(\frac{\partial u_3}{\partial x_2} \right)^2 \right), \tag{41}$$

Table 5
J-integral for a slant crack using (x_1, x_2) and (\bar{x}_1, \bar{x}_2) observer systems.

Observer system (x_1, x_2)					Observer system (\bar{x}_1, \bar{x}_2)			
Transformation law $\begin{bmatrix} J_{\bar{x}_1}^{c\alpha} \\ J_{\bar{x}_2}^{c\alpha} \end{bmatrix} = \begin{bmatrix} \cos \alpha & -\sin \alpha \\ \sin \alpha & \cos \alpha \end{bmatrix} \begin{bmatrix} J_{x_1}^{c\alpha} \\ J_{x_2}^{c\alpha} \end{bmatrix}$								
	$J_{x_1}^{c\alpha}$		$J_{x_2}^{c\alpha}$		$J_{\bar{x}_1}^{c\alpha}$		$J_{\bar{x}_2}^{c\alpha}$	
Inclined angle α	Exact solution $\frac{S^2 \pi a}{2\mu} \cos^2 \alpha$	Dual BEM	Exact solution $\frac{-S^2 a}{\mu} \sin 2\alpha$	Dual BEM	Exact solution $J_{x_1}^{c\alpha} \cos \alpha - J_{x_2}^{c\alpha} \sin \alpha$	Dual BEM	Exact solution $J_{x_1}^{c\alpha} \sin \alpha + J_{x_2}^{c\alpha} \cos \alpha$	Dual BEM
$\alpha = 0$	0.31416	0.31492	0	-0.24e-7	0.31416	0.31492	0	-0.24e-7
$\alpha = \pi/8$	0.26815	0.26881	-0.14142	-0.14175	0.30186	0.30260	-0.02804	-0.02809
$\alpha = \pi/6$	0.23562	0.23620	-0.17321	-0.17361	0.29066	0.29136	-0.03219	-0.03226
$\alpha = \pi/4$	0.15708	0.15746	-0.2	-0.20047	0.25249	0.25310	-0.03035	-0.03041
$\alpha = \pi/3$	0.07854	0.07873	-0.17321	-0.17361	0.18927	0.18972	-0.01859	-0.01862
$\alpha = \pi/2$	0.0	0.164e-16	0	-0.149e-16	0	-0.501e-17	0	0.260e-17
	$(J_{x_1}^{c\alpha})^2 + (J_{x_2}^{c\alpha})^2$				$(J_{\bar{x}_1}^{c\alpha})^2 + (J_{\bar{x}_2}^{c\alpha})^2$			
Inclined angle α	Exact solution $\left(\frac{S^2 \pi a}{2\mu} \cos^2 \alpha\right)^2 + \left(\frac{-S^2 a}{\mu} \sin 2\alpha\right)^2$			Dual BEM	Exact solution $(J_{x_1}^{c\alpha} \cos \alpha - J_{x_2}^{c\alpha} \sin \alpha)^2 + (J_{x_1}^{c\alpha} \sin \alpha + J_{x_2}^{c\alpha} \cos \alpha)^2$			Dual BEM
$\alpha = 0$	0.09870			0.09917	0.09870			0.09917
$\alpha = \pi/8$	0.09190			0.09235	0.09190			0.09235
$\alpha = \pi/6$	0.08552			0.08593	0.08552			0.08593
$\alpha = \pi/4$	0.06467			0.06498	0.06467			0.06498
$\alpha = \pi/3$	0.03617			0.03634	0.03617			0.03634
$\alpha = \pi/2$	0			0.272e-34	0			0.319e-35

$$T_3 = \sigma_{13}n_1 + \sigma_{23}n_2 = \mu \left(\frac{\partial u_3}{\partial x_1} \cos \beta + \frac{\partial u_3}{\partial x_2} \sin \beta \right), \quad (42)$$

respectively. Therefore, we have

$$J_{x_1}^{i\alpha} = \int_{\Gamma} \frac{\mu}{2} \left(-\left(\frac{\partial u_3}{\partial x_1}\right)^2 \cos \beta + \left(\frac{\partial u_3}{\partial x_2}\right)^2 \cos \beta - 2 \frac{\partial u_3}{\partial x_1} \frac{\partial u_3}{\partial x_2} \sin \beta \right) d\Gamma, \quad (43)$$

$$J_{x_2}^{i\alpha} = \int_{\Gamma} \frac{\mu}{2} \left(\left(\frac{\partial u_3}{\partial x_1}\right)^2 \sin \beta - \left(\frac{\partial u_3}{\partial x_2}\right)^2 \sin \beta - 2 \frac{\partial u_3}{\partial x_1} \frac{\partial u_3}{\partial x_2} \cos \beta \right) d\Gamma. \quad (44)$$

For the (\bar{x}_1, \bar{x}_2) observer system as shown in Table 4(b), the normal vector of integral-path is

$$\bar{n} = (\cos(\alpha + \beta), \sin(\alpha + \beta)). \quad (45)$$

The strain energy density and the traction along Γ are

$$\bar{W} = \frac{\bar{\sigma}_{13}^2 + \bar{\sigma}_{23}^2}{2\mu} = \frac{\mu}{2} \left(\left(\frac{\partial \bar{u}_3}{\partial \bar{x}_1}\right)^2 + \left(\frac{\partial \bar{u}_3}{\partial \bar{x}_2}\right)^2 \right), \quad (46)$$

$$\bar{T}_3 = \bar{\sigma}_{13}\bar{n}_1 + \bar{\sigma}_{23}\bar{n}_2 = \mu \left(\frac{\partial u_3}{\partial x_1} \cos \beta + \frac{\partial u_3}{\partial x_2} \sin \beta \right), \quad (47)$$

respectively. The *J*-integral yields

$$J_{\bar{x}_1}^{i\alpha} = \int_{\Gamma} \frac{\mu}{2} \left(-\left(\frac{\partial u_3}{\partial x_1}\right)^2 \cos(\beta - \alpha) + \left(\frac{\partial u_3}{\partial x_2}\right)^2 \cos(\beta - \alpha) - 2 \frac{\partial u_3}{\partial x_1} \frac{\partial u_3}{\partial x_2} \sin(\beta - \alpha) \right) d\Gamma, \quad (48)$$

$$J_{\bar{x}_2}^{i\alpha} = \int_{\Gamma} \frac{\mu}{2} \left(\left(\frac{\partial u_3}{\partial x_1}\right)^2 \sin(\beta - \alpha) - \left(\frac{\partial u_3}{\partial x_2}\right)^2 \sin(\beta - \alpha) - 2 \frac{\partial u_3}{\partial x_1} \frac{\partial u_3}{\partial x_2} \cos(\beta - \alpha) \right) d\Gamma. \quad (49)$$

Table 6
J-integral for a slant rigid-line inclusion using (x_1, x_2) and (\bar{x}_1, \bar{x}_2) observer systems.

Observer system (x_1, x_2)					Observer system (\bar{x}_1, \bar{x}_2)				
Transformation law $\begin{bmatrix} J_{x_1}^{i\alpha} \\ J_{x_2}^{i\alpha} \end{bmatrix} = \begin{bmatrix} \cos \alpha & -\sin \alpha \\ \sin \alpha & \cos \alpha \end{bmatrix} \begin{bmatrix} J_{X_1}^{i\alpha} \\ J_{X_2}^{i\alpha} \end{bmatrix}$									
	$J_{x_1}^{i\alpha}$		$J_{x_2}^{i\alpha}$			$J_{\bar{x}_1}^{i\alpha}$		$J_{\bar{x}_2}^{i\alpha}$	
Inclined angle α	Exact solution $-\frac{S^2 \pi a}{2\mu} \cos^2 \alpha$	Dual BEM	Exact solution $\frac{S^2 a}{\mu} \sin 2\alpha$	Dual BEM	Exact solution $J_{x_1}^{i\alpha} \cos \alpha - J_{x_2}^{i\alpha} \sin \alpha$	Dual BEM	Exact solution $J_{\bar{x}_1}^{i\alpha} \sin \alpha + J_{\bar{x}_2}^{i\alpha} \cos \alpha$	Dual BEM	Dual BEM
$\alpha = 0$	-0.31416	-0.31254	0	-1.38e-7	-0.31416	-0.31254	0	-1.38e-8	
$\alpha = \pi / 8$	-0.26815	-0.26677	0.14142	0.14078	-0.30186	-0.30025	0.02804	0.02775	
$\alpha = \pi / 6$	-0.23562	-0.23441	0.17321	0.17243	-0.29066	-0.28908	0.03219	0.03178	
$\alpha = \pi / 4$	-0.15708	-0.15627	0.2	0.19910	-0.25249	-0.25112	0.03035	0.02967	
$\alpha = \pi / 3$	-0.07854	-0.07814	0.17321	0.17242	-0.18927	-0.18837	0.01859	0.01773	
$\alpha = \pi / 2$	0.0	-0.26e-17	0	0.17e-16	0	0.19e-16	0	0.43e-17	
	$(J_{x_1}^{i\alpha})^2 + (J_{x_2}^{i\alpha})^2$					$(J_{\bar{x}_1}^{i\alpha})^2 + (J_{\bar{x}_2}^{i\alpha})^2$			
Inclined angle α	Exact solution $\left(\frac{-S^2 \pi a}{2\mu} \cos^2 \alpha \right)^2 + \left(\frac{S^2 a}{\mu} \sin 2\alpha \right)^2$			Dual BEM	Exact solution $(J_{x_1}^{i\alpha} \cos \alpha - J_{x_2}^{i\alpha} \sin \alpha)^2 + (J_{x_1}^{i\alpha} \sin \alpha + J_{x_2}^{i\alpha} \cos \alpha)^2$			Dual BEM	
$\alpha = 0$	0.09870			0.09768	0.09870			0.09768	
$\alpha = \pi / 8$	0.09190			0.09099	0.09190			0.09092	
$\alpha = \pi / 6$	0.08552			0.08468	0.08552			0.08458	
$\alpha = \pi / 4$	0.06467			0.06406	0.06467			0.06394	
$\alpha = \pi / 3$	0.03617			0.03583	0.03617			0.03580	
$\alpha = \pi / 2$	0			0.31E-35	0			0.36E-35	

where $S = 1$, $\mu = 1$, $a = 0.2$, $J_{x_1}^{c\alpha} = \int_{\Gamma} W n_1 - T_3 \frac{\partial u_3}{\partial x_1} d\Gamma$, $J_{x_2}^{c\alpha} = \int_{\Gamma} W n_2 - T_3 \frac{\partial u_3}{\partial x_2} d\Gamma$, $J_{\bar{x}_1}^{c\alpha} = \int_{\Gamma} \bar{W} \bar{n}_1 - \bar{T}_3 \frac{\partial \bar{u}_3}{\partial \bar{x}_1} d\Gamma$, $J_{\bar{x}_2}^{c\alpha} = \int_{\Gamma} \bar{W} \bar{n}_2 - \bar{T}_3 \frac{\partial \bar{u}_3}{\partial \bar{x}_2} d\Gamma$.

The transformation law between the two observer systems is constructed in Table 4. We also find that the total displacement, $u_3(x_1, x_2)$, $\bar{u}_3(\bar{x}_1, \bar{x}_2)$, strain energy density, W , \bar{W} , and the traction, T_3 , \bar{T}_3 , are invariants no matter that which plane observer system is used. Table 4 gives

$$\begin{bmatrix} \frac{\partial \bar{u}_3}{\partial \bar{x}_1} \\ \frac{\partial \bar{u}_3}{\partial \bar{x}_2} \end{bmatrix} = \begin{bmatrix} \cos \alpha & -\sin \alpha \\ \sin \alpha & \cos \alpha \end{bmatrix} \begin{bmatrix} \frac{\partial u_3}{\partial x_1} \\ \frac{\partial u_3}{\partial x_2} \end{bmatrix}, \tag{50}$$

$$\begin{bmatrix} \bar{\sigma}_{13} \\ \bar{\sigma}_{23} \end{bmatrix} = \begin{bmatrix} \cos \alpha & -\sin \alpha \\ \sin \alpha & \cos \alpha \end{bmatrix} \begin{bmatrix} \sigma_{13} \\ \sigma_{23} \end{bmatrix}, \tag{51}$$

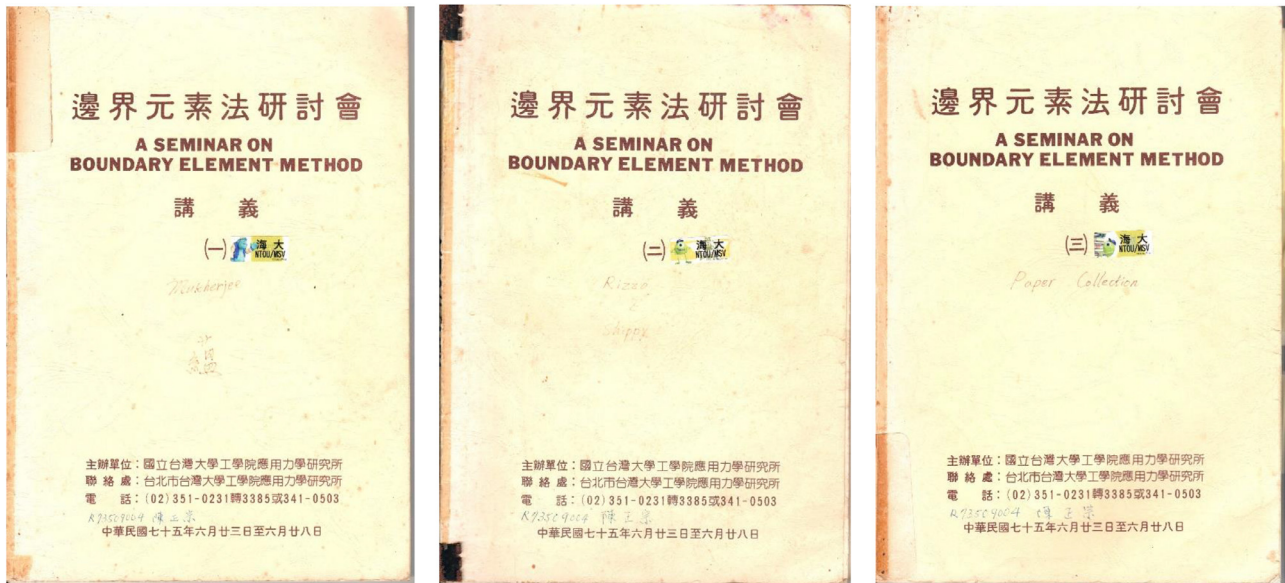
$$\begin{bmatrix} \bar{n}_1 \\ \bar{n}_2 \end{bmatrix} = \begin{bmatrix} \cos \alpha & -\sin \alpha \\ \sin \alpha & \cos \alpha \end{bmatrix} \begin{bmatrix} n_1 \\ n_2 \end{bmatrix}, \tag{52}$$

$$\begin{bmatrix} J_{\bar{x}_1}^{i\alpha} \\ J_{\bar{x}_2}^{i\alpha} \end{bmatrix} = \begin{bmatrix} \cos \alpha & -\sin \alpha \\ \sin \alpha & \cos \alpha \end{bmatrix} \begin{bmatrix} J_{x_1}^{i\alpha} \\ J_{x_2}^{i\alpha} \end{bmatrix}. \tag{53}$$

From Eq. (53), we realize that the relation of the *J*-integral derived by different observer systems is a rotation matrix. Finally, the length of the vector is an invariant as shown below:

$$(J_{x_1}^{i\alpha})^2 + (J_{x_2}^{i\alpha})^2 = (J_{\bar{x}_1}^{i\alpha})^2 + (J_{\bar{x}_2}^{i\alpha})^2. \tag{54}$$

It indicates that the *J*-integral defined by Rice is not invariant and is only one component of a vector. To demonstrate the first order tensor of *J*-integral, two cases, one crack and one rigid-line inclusion, are given. The comparison of the exact solution and numerical results by using the dual BEM are shown in Tables 5 and 6 for a slant crack and a slant rigid-line inclusion, respectively. It is found that the two components of the vector obey the transformation law in the results of the dual BEM. Table 5 also shows that $(J_{x_1}^{c\alpha})^2 + (J_{x_2}^{c\alpha})^2$, $(J_{\bar{x}_1}^{c\alpha})^2 + (J_{\bar{x}_2}^{c\alpha})^2$, $J_{x_1}^{c\alpha}$ and $J_{x_2}^{c\alpha}$ decrease when the inclined angle α increases. Table 6 also shows that $(J_{x_1}^{i\alpha})^2 + (J_{x_2}^{i\alpha})^2$ decrease and $J_{x_1}^{c\alpha}$ and $J_{\bar{x}_1}^{i\alpha}$ increase when the inclined an-



(a) First part

(b) Second part

(c) Third part

Fig. 5. Three proceedings for the seminar on the boundary element method in Taiwan by Prof. Rizzo.



Fig. 6. Group photos of Taiwan BEM/Meshless meetings since 2010. The 11th BEM meetings was held on Oct. 17, National Taiwan Ocean University, 2020.

History & Background Taiwan BEM workshop (1986-2020)					
Year	The host unit	The organizer		Ceremony	(BEM 11)
1986	NTU IAM		Prof. Y H Pao	Establishment of NTU IAM	 Prof. F J Rizzo
1989	NTU		Prof. D L Young	NSC	 Prof. J A Liggett
1998	NSC		Prof. J T Chen	NCHC	 Prof. A H D Cheng
2010	NTOU-HRE-MSV		Prof. J T Chen	NTOU-HRE 50th anniversary 	 Prof. Z C Li
2011	NCTS(South)		Prof. K M Lee	NCKU 80th anniversary 	NCKU
2012	Feng Chia University		Prof. Y C Shiah	Prof. Hong's 60th birthday	 Prof. H-K Hong
2013	National Chung Hsing University		Prof. K J Shou	Congratulations for Academician	 Dean S L Crouch Academician,NAE
2014	National SYS University		Prof. T T Lu	Prof. Young's 70th birthday	 Prof. D L Young
2015	NCREE (cross strait)		Dr. R Z Wang	NCREE	Cross strait ceremony
2016	NCTS (Japan-Taiwan)		Prof. J H Lee	NCTS	 Prof. H-K Hong  Prof. W-W Lin
2017	NIU	 	Prof. I L Chern Prof. K H Chen	Ilan Univ.	 Prof. H-K Hong  Prof. W-C Wang
2018	ISU	 	Prof. H T Huang Prof. I L Chen	Iso Univ.	 Prof. D L Young
2019	NCKU		Prof. L W Liu	Cheng Kung Univ.	 Prof. J T Chen
2020	NTOU	 	Prof. Y T Lee Prof. C M Fan	NTOU-HRE 60th anniversary 	 Prof. C B Hwu

Fig. 7. The history of Taiwan BEM workshop since 1986.

gle α increases. Both results indicate that the SIF reaches its maximum when $\alpha = 0$ and $\alpha = \pi$.

5. Conclusions

In this paper, we derived the J -integral for the slant crack and slant rigid-line inclusion under the anti-plane shear. Thanks to the degenerate kernel, the path independence of the J -integral was analytically examined. The positive and negative J -integrals for the slant crack and the slant rigid-line inclusion, respectively, were also theoretically derived. The numerical evidences were numerically calculated by using the dual BEM. Besides, we found that J -integral was not an invariant and was a component of the first direction of a vector although it is path independent. The first order tensor of J -integral was theoretically and numerically verified to satisfy the transformation law for the slant crack or slant rigid-line inclusion subjected to two different observer systems.

6. Remarks for the Rizzo special issue

In 1986, Prof. Y H Pao, a teacher of the first author, invited Prof. Rizzo to give a BEM workshop in Institute of Applied Mechanics, Taiwan University. During that week, June 23 to 28, the first author was Prof. Rizzo's TA to prepare the execution files of his Fortran files. Prof. Shippy and Mukherjee also accompanied with Prof. Rizzo to have lectures. Now, three proceedings for the seminar on boundary element method are still on the desk of the first author as shown in Fig. 5. Prof. Rizzo said that he enjoyed a good time like a king in Taiwan. At the same time, Prof.

H-K Hong and the first author developed the dual BIEM/BEM for problems containing degenerate boundaries using the hypersingular equation. This article is also an extension work of the dual BEM. We appreciated very much that Prof. Rizzo stimulated the BEM research at that time in Taiwan. Since 1986, many researchers paid attention to BEM study in Taiwan. A series domestic meeting was open since 2010, the 11th annual BEM meeting was held in National Taiwan Ocean University, Keelung, 2020. The group photo is shown in Fig. 6. Besides, the organizer and plenary lecturer are also given in Fig. 7. Now the BEM power of Taiwan is Top 5 country in the world.

Declaration of Competing Interest

None.

Acknowledgments

The authors wish to thank the financial support from the Ministry of Science and Technology, Taiwan under Grant No. MOST 109-2221-E-019-001-MY3.

References

- [1] Hong HK, Chen JT. Derivations of integral equations of elasticity. ASCE J Eng Mech 1988;114:1028–44.
- [2] England AH. On stress singularities in linear elasticity. Int J Eng Sci 1971;9:571–85.
- [3] Chen YZ, Hasebe N. An alternative Fredholm integral equation approach for multiple crack problem and multiple rigid line problem in plane elasticity. Eng Fract Mech 1992;43(2):257–68.

- [4] Dong CY, Lee KY. Numerical analysis of doubly periodic array of cracks/rigid-line inclusions in an infinite isotropic medium using the boundary integral equation method. *Int J Fract* 2005;133:389–405.
- [5] Liu YJ, Nishimura N, Otani Y, Takahashi T, Chen X L, Munakata H. A fast boundary element method for the analysis of fiber-reinforced composites based on a rigid-inclusion model. *ASME J Appl Mech* 2005;72(1):115–28.
- [6] Dong CY. The integral equation formulations of an infinite elastic medium containing inclusions, cracks and rigid lines. *Eng Fract Mech* 2008;75(13):3952–65.
- [7] Mirsalimov VM, Hasanov FF. Nucleation of cracks in an isotropic medium with periodic system of rigid inclusions under transverse shear. *Acta Mech* 2015;226(2):385–95.
- [8] Rudoy E. On numerical solving a rigid inclusions problem in 2D elasticity. *Z Angew Math Phys* 2017;68(19).
- [9] Dong CY, Lo SH, Cheung YK. Interaction between cracks and rigid-line inclusions by an integral equation approach. *Comput Mech* 2003;31:238–52.
- [10] Xiao JH, Xu YL, Zhang FC. Interaction between periodic cracks and periodic rigid-line inclusions in piezoelectric materials. *Acta Mech* 2013;224:777–87.
- [11] Wang ZY, Zhang HT, Chou YT. Characteristics of the elastic field of a rigid line inhomogeneity. *ASME J Appl Mech* 1985;52(4):818–22.
- [12] Rice JR. A path independent integral and the approximate analysis of strain concentration by notches and cracks. *ASME J Appl Mech* 1968;35(2):379–86.
- [13] Chen JT, Kao JH, Huang YL, Kao SK. On the stress concentration factor of circular/elliptic hole and rigid inclusion under the remote anti-plane shear by using degenerate kernels. *Arch Appl Mech* 2021.
- [14] Lee YT, Chen JT, Kuo SR. Semi-analytical approach for torsion problems of a circular bar containing multiple holes and/or cracks. *Eng Fract Mech* 2019;219:106547.
- [15] Hellan K. Introduction to fracture mechanics. New York: McGraw Hill; 1984.
- [16] Nishioka T. Invariance of the elastodynamic J integral (J^*), with respect to the shape of an infinitesimal process zone. *Eng Fract Mech* 1989;32(2):309–19.
- [17] Bazhenov VA, Gulyar AI, Piskunov SO, Sakharov AS, Shkriil AA. Method to evaluate the J integral in finite element models of prismatic bodies. *Int Appl Mech* 2008;44(12):1378–88.
- [18] Chen JT, Kao JH, Huang YL, Kao SK. Study on the stress intensity factor and the double-degeneracy mechanism in the BEM/BIEM for anti-plane shear problems. *Theor Appl Fract Mech* 2021;112.
- [19] Morse PM, Feshbach H. Methods of theoretical physics. New York: McGraw-Hill; 1978.
- [20] Chen JT, Lee YT, Lee JW. Torsional rigidity of an elliptic bar with multiple elliptical inclusions using a null-field integral approach. *Comput Mech* 2010;46:511–19.
- [21] Lee YT, Chen JT. Null-field approach for the antiplane problem with elliptical holes and/or inclusions. *Compos B Eng* 2013;44:283–94.
- [22] Irwin GR. Analysis of stresses and strains near the end of a crack traversing a plate. *ASME J Appl Mech-T* 1957;24:361–4.
- [23] Wang YH. SIF calculation of an internal crack problem under anti-plane shear. *Comput Struct* 1993;48(2):291–5.
- [24] Banks-Sills L. J-integral for Mode-III from book. *Problems of Fracture Mechanics and Fatigue: A Solution Guide*; 2003. p. 219–22.
- [25] Gdoutos EE, Rodopoulos CA, Yates JR. *Problems of Fracture Mechanics and Fatigue: A Solution Guide*. New York: Springer-Verlag; 2003.
- [26] Sun CT, Jin ZH. *Fracture Mechanics*. United States: Academic Press; 2011.
- [27] Corso FD, Shahzad S, Bigoni D. Isotoxal star-shaped polygonal voids and rigid inclusions in nonuniform antiplane shear fields. Part I: formulation and full-field solution. *Int J Solids Struct* 2016;85-86:67–75.
- [28] Shahzad S, Niiranen J. Analytical solution with validity analysis for an elliptical void and a rigid inclusion under uniform or nonuniform anti-plane loading. *Theor Appl Fract Mech* 2018;97:62–72.
- [29] Chen JT, Huang WS, Lee YT, Kao SK. A necessary and sufficient BEM/BIEM for two-dimensional elasticity problems. *Eng Anal Bound Elem* 2016;67:108–14.
- [30] Chen JT, Huang WS, Lee YT, Kuo SR, Kao SK. Revisit of degenerate scales in the BIEM/BEM for 2D elasticity problems. *Mech Adv Mater Struct* 2017;24(1):1–15.